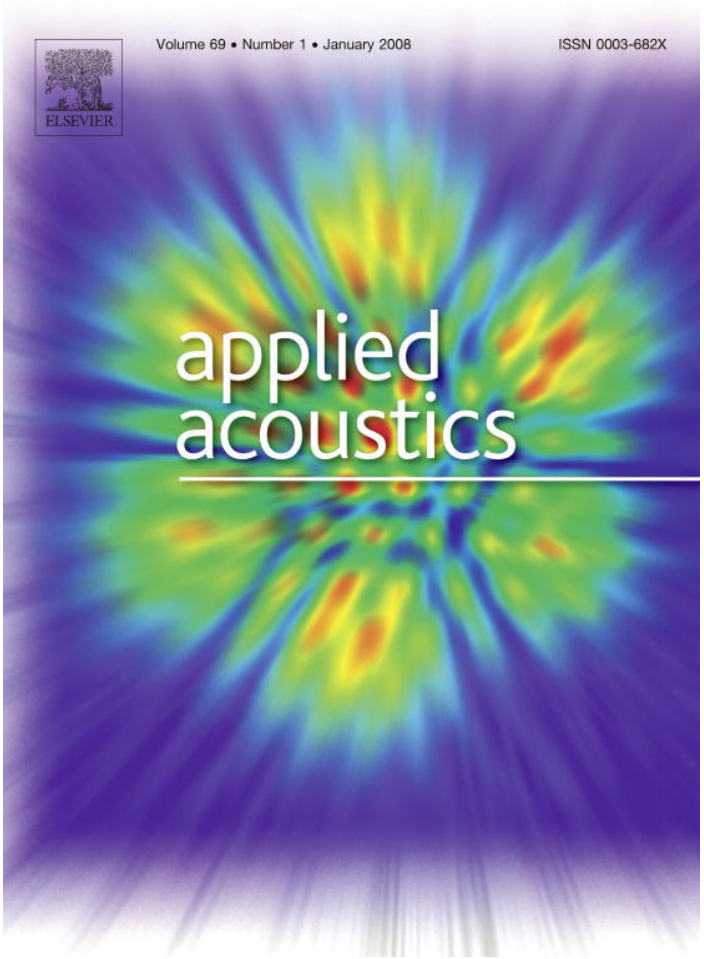

Available online at www.sciencedirect.com
ScienceDirect
Applied Acoustics 69 (2008) 47–59
applied acoustics
www.elsevier.com/locate/apacoust

Model and estimation method for predicting the sound radiated by a horn loudspeaker – With application to a car horn

Guillaume Lemaitre [a,c,*], Boris Letinturier [b], Bruno Gazengel [c]

[a] IRCAM – Sound Perception and Design team, F-75004 Paris, France
[b] SCE-Klaxon, 106 ZI du Clos de la Reine, F-78410 Aubergenville, France
[c] Laboratoire d'Acoustique, de l'Université du Maine, F-72000 Le Mans, France

Received 16 December 2005; received in revised form 13 October 2006; accepted 16 October 2006
Available online 1 December 2006

Abstract

This paper deals with a new car horn device made of a sound synthesizer and an electrodynamic horn loudspeaker. It presents an one-dimensional model allowing to predict the loudspeaker efficiency and a specific method to estimate experimentally the model parameters. First, this model aims at reducing the time spent in the design process. Second it aims at correcting the sound emitted by the sound synthesizer in order that the listener hears the sound designed for creating the warning message. The study gives a survey of the vast loudspeaker literature. It is based on the conventional electroacoustic approach used for electrodynamic loudspeakers and on wave propagation models used for characterizing acoustic horns. The estimation of the model parameter values is performed using measurements of the electrical impedance of the loudspeaker and of the acoustic impedance of the horn. The model is assessed by comparing the calculated and measured electrical impedances and horn efficiencies. Results show that the model predicts well the horn efficiency up to 2500 Hz, the limitation being due to the horn radiation impedance modelization.

PACS: 43.38.Dv; 43.38.Ja; 43.38.Tj

Keywords: Horn loudspeaker modelization; Parameter estimation method

1. Introduction

Nowadays, automotive industry is paying more and more attention to the sounds emitted by cars, and especially to the sounds of car horns, which can be a deciding factor for potential car buyers. The aim of manufacturers is now to design different car horns for different cars, just as they already design many other sounds such as this of a closing door. Yet car horns are peculiar, since they must address a warning message to the road users [1]. Thus car horn builders have to design sounds that fulfill the car builders wishes, and at the same time they must ensure that these sounds are understood as danger signals.

Car horns have been built up to now using electromagnetic excitors coupled together with acoustical (horn) or mechanical resonators (disk). Unfortunately, these technologies do not enable to design new sounds, unless the horn builder adapts the resonator. Hence, a new device has been designed, made of a synthesizer and of an electrodynamic horn loudspeaker. The electrodynamic loudspeaker has been used for many years to provide audio signals and has shown its capability in reproducing many different sounds (see [2] for a review).

* Corresponding author. Address: IRCAM – Sound Perception and Design team, 1 Place Stravinsky, F-75004 Paris, France. Tel./fax: +33 492 385083.
E-mail addresses: Guillaume.Lemaitre@ircam.fr (G. Lemaitre), Boris.Letinturier@sce-klaxon.com (B. Letinturier), bruno.gazengel@univ-lemans.fr (B. Gazengel).

0003-682X/$ - see front matter © 2006 Elsevier Ltd. All rights reserved.
doi:10.1016/j.apacoust.2006.10.005

In previous studies [3–5], we have defined acoustic requirements that allow synthesized sounds to be associated with the warning message. But because of the loudspeaker response, the sounds heard by road-users may be fairly different from the laboratory fine-designed sounds. Moreover, the horn must meet particular requirements concerning the acoustic level (105 dB(A) at 2 m). Hence, the loudspeaker behavior has to be integrated along the design process: sound designers need a physical model of the loudspeaker to anticipate the sound modifications, and loudspeaker designers need a physical model to make the loudspeaker compatible with the signal requirements.

The purpose of the study is first to provide with a model of the horn loudspeaker made of an electrodynamic driver coupled together with an acoustic horn. A huge amount of studies dealing whether with electrodynamical loudspeakers or with horn propagation have been presented. On this basis, we propose a global model of the horn loudspeaker and we define a parameter estimation method. This method is designed to be easily implemented in an industrial context. Finally, we assess this physical model in order to define the frequency range in which it can be applied.

In Section 2, we present the state of the art of linear physical models. We also discuss the choice of linear models. In Section 3, we develop the horn loudspeaker model using a quadripole formulation. In Section 4 we present the method used to estimate the values of the input parameters of the model. This method is based on impedance measurements of the loudspeaker loaded with different closed volumes. Then, we characterize experimentally the horn and we assess the uncertainty in the parameter estimation in Section 5. Finally, we discuss the limits of the physical model in Section 6.

2. State of the art

The car horn is made of an electrodynamical driver coupled together with a compression chamber and an acoustic horn (see Fig. 1). There are two families of physical model for such systems: the linear and the non-linear models. Linear models enable to describe the horn loudspeaker as a four-pole system, the characteristics of which depend on frequency. Non-linear models take into account the non-linearity of the driver (see [6–8]) and the non-linear propagation of sound in the compression chamber and in the horn (see [9] for a review). In the case of horn loudspeaker, non-linearities in the horn are the major cause of distortion [10]. Global non-linear models of horn loudspeakers have been proposed in e.g. [11]. These models are very complex and thus allow to finely shape the response of the device by means of feedback or feed-forward control systems (e.g. in order to reduce distortion). However, they can not lead to simple device design modifications, since they hardly allow to identify which mechanical or electrical cause is responsible for the observed distortions. Moreover, they are hardly usable in an industrial context, because of the careful need of parameter estimation. For these reasons, we decide to use a linear model of the loudspeaker. The following paragraphs present a state of the art of linear models of loudspeaker and horns.

2.1. Direct radiation loudspeaker models

Most of studies dealing with electrodynamic loudspeaker models are based on the so-called *Thiele and Small's model*. This model results from the work of Thiele first published in 1961 [12], formalized and popularized ten years after by Small [13,14]. Some work had already been done before on the basis of Beranek's [15] and Olson's [16] studies, but Thiele and Small's model had the advantages of both simplicity and accuracy, and shortly became a standard.

This model is a lumped-elements electroacoustical model. Each part of the loudspeaker (voice coil, moving element, diaphragm, etc.) is modelized with an electrical analogy (resistor, capacitor, etc.). It allows to predict the loudspeaker efficiency (radiated acoustical power as a func-

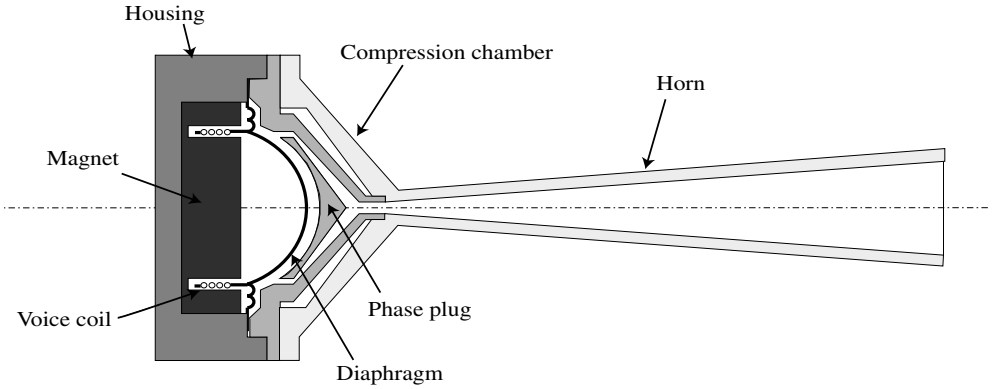

Fig. 1. Cross-section vue of the loudspeaker.

tion of electrical power)[1] and hence to assess the influence of each component.

Although this model is defined by a few parameters, the experimental accurate estimation of these parameters may be difficult. For a long time, parameters have been estimated from loudspeaker frequency response properties (resonance frequencies, damping factor, etc.) [17]. Since early 80s, however improvements of computers have made global model fitting techniques possible. The basic principle is to run an error minimization algorithm between the measured and the predicted response. The extreme case is to model the loudspeaker as a two-port "black box". Experimental procedures and curve fitting techniques amounts then in measuring the elements of the two-port model, without any link to the physical constitutive elements of the loudspeaker. Such methods are of very common use for non-linear models (see for example [18]), and have also been used for linear models [19–21]. Their predictions are much more accurate, but they can not lead to design specifications.

Thiele and Small's model is based on some physical simplifications (lumped element hypothesis) that let the model fail to predict fine and high frequency phenomena. Further work has aimed at improving the fine modelization of each element. The influence of the diaphragm shape and of the resonance modes have been studied in, e.g. [22]. Electrical phenomena within the voice coil (such as Eddy current) have been studied and modelized in [23]. Suspension modelization was improved by Knudsen and Jensen [24].

There exists some other studies that have been developed parallel to Thiele and Small's model [25]. They propose much more precise and physically grounded models of the mechanical part of the loudspeaker. But these models can no longer be described by lumped-element circuits. Their predictions are much accurate than Thiele and Small's models, but their complexity, and the very delicate parameter estimation protocols made them very difficult to use in an industrial application.

2.2. Horn loudspeakers

The propagation of acoustic waves in horns have been principally described in musical acoustics studies. Acoustical propagation in horn is described in Nederveen's [26] reference book. The formulation used in most of electroacoustical studies is summarized in [16].

2.2.1. Acoustic propagation in waveguides

The fundamental equation describing wave propagation in variable section waveguides is the *Webster equation* [27,28]. It allows to express the relationship between input (*throat* of the horn) and output (*mouth* of the horn) quantities: acoustic pressure and volume velocity. Hence one boundary condition (the radiating impedance at horn mouth) is required for solving the system. Computing radiation impedance in the general case is a very complex problem. Levine and Schwinger [29] give a complex analytical expression for a cylindrical pipe radiating in an infinite space. Useful approximations are given by Caussé et al. [30], Dalmont et al. [31] (based on Norris and Sheng's work [32]), and Hélie and Rodet [33].

Dealing with the wave propagation, several approaches are available. First, a horn can be described in the frequency domain by its throat impedance (or equivalently by transmission matrices). An usual assumption is that waves propagating along the horns are either plane or spherical, but Benade and Jansson [34,35] showed that because of axial to radial mode conversion, none of this hypotheses is fairly true. However, a fruitful approach has been introduced by Plitnik and Strong [36]. It consists in numerizing any bore geometry by a series of cylinders. Caussé et al. [30] further generalized this method to include viscothermal losses. A same approach is used by Holland et al. [37] for the loudspeaker horn. They numerize the horn as a series of exponential elements, taking axial to radial mode conversion into account. Another approach is to modelize the horn with an electroacoustical circuit [38]. Finally, wave propagation can be described in the time domain. This approach has been used for real-time simulation of musical instruments (see e.g. [39]).

2.2.2. Loudspeaker horns

Loudspeaker horns allow to adapt impedance between the diaphragm and the propagation medium. They force the diaphragm movements to remain small, and they maximize the amount of energy radiated to the medium [40,41]. Attempts to optimize energy transmission has lead to new geometries of horns [42].

Horns have a strong directivity, that may greatly varies with frequency. Conical horns are known to be the simplest bore geometry allowing an uniform directivity [43]. But this hypothesis is valid only below a particular frequency ("break wave number") [42]. Several horn geometries have then been proposed to control directivity over a large frequency range [44].

Horns are most of the times coupled together with the loudspeaker diaphragm by means of an element called the *compression chamber*. This element aims at adaptating impedance between a large diaphragm radius and a smaller horn throat radius. Its specific inside geometry (*the phase plug*) is designed to cancel radial modes at throat [45], which would under-optimize energy transmission into the horn. An electroacoustical model has been proposed by Henricksen [46].

Finally, only a few studies has been published for proposing a global model of a horn loudspeaker. Leach [47] proposed a global electroacoustical model of an exponential horn loudspeaker, and demonstrated its band-pass filter behavior. Geddes and Clark [48] published a rather complex global model, with a specific resolution of the

[1] Note that this definition of *efficiency* is not this one proposed by Thiele [12]. It rather corresponds to *sensitivity*, in the case of a microphone.

Webster equation. Their predictions fitted measures very well.

3. Horn loudspeaker model

3.1. Description of the loudspeaker

The loudspeaker under study is made of three parts: an electrical to mechanical transducing system (the voice coil within the magnetic field), a mechanical part (the moving element, made of the suspended diaphragm and coil), and an acoustical load (compression chamber and horn). The two former parts define the electrodynamic driver, while the latter part defines the resonator (see Fig. 1).

3.2. General formulation of the problem

Assuming a 1-D propagation model, the horn can be represented by an equivalent electrical circuit shown in Fig. 2 (see Tables A.1 and A.2 in Appendix A for a glossary of symbols). Formally the problem is defined by four independant variables (u_g, i_g, p_d, q_d), which represent respectively the input voltage and current, the acoustic pressure in front of the diaphragm and the volume velocity generated by the diaphragm. They are linked together by

$$\begin{bmatrix} u_g \\ i_g \end{bmatrix} = \begin{bmatrix} \frac{S_d}{Bl} Z_{ec} & \frac{Bl}{S_d}\left(1 + \frac{Z_{ec}}{Z_{em}}\right) \\ \frac{S_d}{Bl} & \frac{Bl}{S_d}\frac{1}{Z_{em}} \end{bmatrix} \begin{bmatrix} p_d \\ q_d \end{bmatrix}, \tag{1}$$

where S_d is the effective surface of the diaphragm, Bl the force factor, Z_{ec} the electrical voice coil impedance, $Z_{em} = Bl^2/Z_{mm}$ the motional impedance (written in the electrical analogy), and Z_{mm} is the motional impedance written in the mechanical analogy. The relation between the acoustic pressure p_d and acoustic volume velocity q_d is given by

$$\frac{p_d}{q_d} = Z_{al}, \tag{2}$$

where Z_{al} is the acoustical load impedance which represents the boundary condition. The pressure radiated at horn mouth p_m is given by

$$\frac{p_m}{p_d} = T^{load}, \tag{3}$$

where T^{load} is the transmission matrix of the horn.

The problem is completly defined by the three equations (1)–(3). The following paragraphs develop the formulation of Z_{ec}, Z_{mm}, Z_{al}, and T^{load} corresponding to the electrical, mechanical and acoustical parts of the loudspeakers.

3.3. Voice coil, moving element, and acoustical load

3.3.1. Voice coil

The voice coil is made of a copper winding. The simplest model is a resistance and an inductance connected in series. But many empirical studies have shown that this model fails for high frequencies [12,49,50,23,51]. Vanderkooy has explained this phenomenon by the presence of Eddy currents at the magnet surface [51], and proposed a model to account for these currents ($R_e + K\omega^{1/2} + jK\omega^{1/2}$ impedance behavior). Wright [50] has then proposed to generalize this model, since it was not able to explain some of the reported phenomena at high frequencies, on the basis of empirical measurements ($R_e + K_r\omega^{X_r} + jK_i\omega^{X_i}$ impedance behavior). We adopt a similar empirical model derived to fit our own measurements of the voice coil impedance out of the magnetic field

$$Z_{ec} = R_{ec}(1 + \omega/\omega_r)^r + j(\omega L_{ec})^\alpha, \tag{4}$$

where ω_r, r, and α are empirical parameters which account for the increase of the resistance and of the decrease of the inductance at high frequencies (note that the asymptotic behavior of this model is identical to Wright's).

3.3.2. Moving element

The dome-like loudspeaker diaphragm is suspended to the loudspeaker housing by peripherical corrugations of the membrane. Assuming that the membrane acts like a rigid piston, this moving element can be modelized by a single mechanical mass M_{mm} linked to a mechanical compliance C_{mm} with mechanical losses R_{mm} (Kelvin's model of suspension [24]). The motional impedance in the electrical domain is then

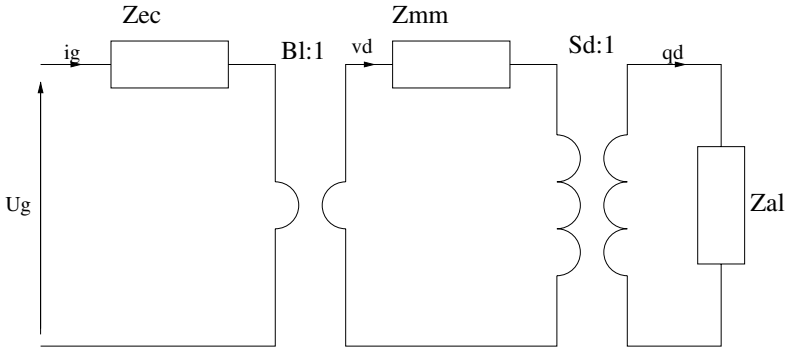

Fig. 2. Equivalent electroacoustical circuit of the loudspeaker.

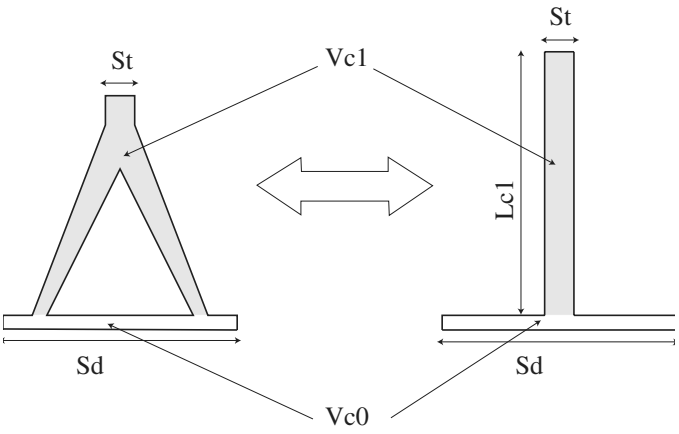

Fig. 3. Geometrical approximation for the compression chamber and the phase plug.

$$Z_{em} = R_{ec}\frac{Q_m}{Q_e}\frac{j\frac{\omega}{\omega_0}Q_m^{-1}}{1+j\frac{\omega}{\omega_0}Q_m^{-1}+(j\frac{\omega}{\omega_0})^2}, \tag{5}$$

where

$$\omega_0 = \frac{1}{\sqrt{M_{mm}C_{mm}}}, \tag{6a}$$

$$Q_m = \frac{1}{R_{mm}C_{mm}\omega_0}, \tag{6b}$$

$$Q_e = \frac{Q_m R_{ec}}{Bl^2/R_{mm}}, \tag{6c}$$

are, respectively, the diaphragm resonance frequency, the mechanical quality factor, and the electrical quality factor.

3.3.3. Acoustical impedance

3.3.3.1. Compression chamber and phase plug. Although there exists some electroacoustical models in the literature [46,48,53], we propose a semi-empirical model of the compression chamber. It is based both on Smith's analytical solution [45] and on geometrical simplifications (see Fig. 3). First, a thin air layer (volume V_{c0}) is compressed between the diaphragm (section S_d) and the phase plug. We modelize it as an acoustical compliance $C_{ac0} = V_{c0}/\rho c^2$. Then waves are propagated along the slits located between the phase plug and the compression chamber walls (annular section S_a): we simplify it in a cylindrical waveguide[2] of section S_t and of length L_{c1}. Finally, waves propagate to the horn throat via a small cylindrical pipe (section S_t, radius r_t).

With this approximation, and after Caussé et al. [30], the input admittance Y_{al} of the compression chamber loaded by an acoustical impedance Z_{at} is given by

$$Y_{al} = \frac{1}{Z_{al}} = jC_{ac0}\omega + \frac{\tanh[jkL_{c1} + a\tanh(\zeta_t/Z_{at})]}{\zeta_t}, \tag{7}$$

where k is the wave number including viscothermal losses at the walls, and ζ_t is the characteristic impedance at the throat. After [54,30], they can be approximated at a temperature of 20 °C by

$$k = \frac{\omega}{c}\left[1 + 3\times10^{-5}\frac{1-j}{2\pi r_t\sqrt{f}} - 3\times10^{-8}\frac{j}{2\pi r_t^2 f}\right], \tag{8a}$$

$$\zeta_t = \frac{\rho c}{S_t}\left[1 + \frac{7.61\times10^{-4}}{r_t\sqrt{f}} - j\frac{4.89\times10^{-6}}{r_t^2 f}\right], \tag{8b}$$

where c is the sound speed and ρ is the air density at rest. The pressure at the compression chamber output (horn throat) p_t is related to the pressure at the diaphragm p_d by

$$\frac{p_t}{p_d} = T^{pipe}(L_{c1}, r_t, Z_{at}) = \frac{1}{\cos(kL_{c1}) + j\zeta_t/Z_{at}\sin(kL_{c1})}. \tag{9}$$

3.3.3.2. Horn. As the cone angles are small, we assume plane wave propagation (for a 20° angle, plane and spherical wave front area are only 1% different). Hence, after [30], acoustical throat impedance Z_{at} of a conical horn loaded by an acoustical mouth radiation impedance Z_{ar} is

$$Z_{at} = \frac{\zeta_t}{\frac{1}{jkx_t} + \tanh\left[jkL + a\tanh\left(\frac{\zeta_m}{Z_{ar}} - \frac{1}{jkx_m}\right)\right]}. \tag{10}$$

Pressure at cone mouth P_m is given as a function of throat pressure P_t by

$$\frac{P_m}{P_t} = T^{horn}(x_t, x_m, L, Z_{ar}) = \frac{x_t}{x_m}\frac{1}{\cos(kL) + j\sin(kL)\left(\frac{\zeta_m}{Z_{ar}} - \frac{1}{jkx_m}\right)}, \tag{11}$$

where x_t, x_m, and L are given in Fig. 4 and are reminded in Table A.2. Wave number k and characteristic impedances ζ_t and ζ_m are given in Eq. (8).

3.3.3.3. Radiation impedance. Radiation impedance models can be found in three studies [30,31,33] dealing with unbaffled radiating waveguides. We use the Dalmont et al. [31] approximation of Levine and Schwinger's [29] and Norris and Sheng's work [32]. Hence the radiation impedance Z_{ar} of an oscillating piston of radius r_m and section S_m is

$$Z_{ar} = \frac{\rho c}{S_m}\frac{1-|R_0|e^{-2jk\delta_0}}{1+|R_0|e^{-2jk\delta_0}}, \tag{12}$$

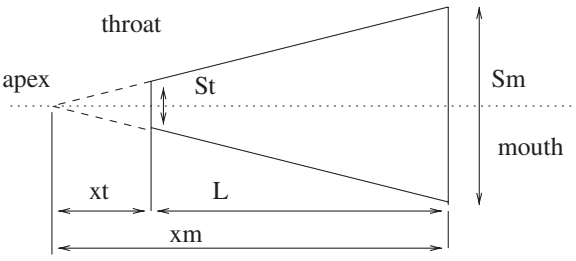

Fig. 4. Conical horn dimensions.

[2] As there are no radial modes, we assume plane wave propagation.

where

$$|R_0| = \frac{1 + 0.2kr_m - 0.084(kr_m)^2}{1 + 0.2kr_m + (0.416(kr_m)^2)}, \tag{13a}$$

$$\delta_0 = 0.6133r_m\left[\frac{1 + 0.44(kr_m)^2}{1 + 0.19(kr_m)^2} - 0.02\sin^2(2kr_m)\right], \tag{13b}$$

and k is defined in Eq. (8).

3.4. Electrical impedance and horn efficiency

Finally, we can derive the electrical impedance and the efficiency of the loudspeaker from the above formulations. From Eq. (1), the loudspeaker electrical input impedance Z_{hp} is

$$Z_{hp} = Z_{ec} + Z_{eM}, \tag{14}$$

where Z_{ec} is the electrical impedance of the voice coil (see Eq. (4)) and $Z_{eM} = (Z_{el}Z_{em})/(Z_{el} + Z_{em})$ is the impedance of the mechano-acoustical load expressed in the electrical domain. Z_{eM} depends on Z_{em} (Eq. (5)) and on $Z_{el} = Bl/(S_d^2 Z_{al})$ (see Eqs. (7), (10), and (12)).

Combining Eqs. (1), (9), and (11) allows to derive the loudspeaker efficiency

$$\frac{p_m}{u_g} = Z_{al}\frac{S_d}{Bl} \times \frac{Z_{eM}}{Z_{ec} + Z_{eM}} T^{pipe}(L_{c1}, r_t, Z_t)T^{horn}(x_t, x_m, L, Z_{ar}), \tag{15}$$

where the total acoustic load impedance Z_{al} is defined by Eqs. (7), (10), and (12), the coil impedance Z_{ec} is defined by Eq. (4), the pipe and horn transmission functions T^{pipe}-(L_{c1}, r_t, Z_g) and $T^{horn}(x_t, x_m, L, Z_{ar})$ are defined by Eqs. (9) and (11).

4. Parameter estimation method

The loudspeaker model presented in Section 3 is defined by 14 parameters: the coupling factors ratio S_d/Bl, the voice coil parameters (R_{ec}, L_{ec}, ω_r, r, and α), the moving element parameters (ω_0, Q_m, and Q_e) and the acoustic load parameters (V_{c0}, L_{c1}, r_t, r_m, and L).

The usual methods used to estimate the driver parameters imply to measure the electrical impedance when the diaphragm is freely radiating. This not possible in our case, since the diaphragm is fixed to the housing by the compression chamber. We have measured that unmounting the compression chamber (to let the diaphragm freely radiating), and then remounting it changes dramatically the mechanical parameter values. Thus our method consists first in measuring the horn and compression chamber input acoustical impedances for the compression chamber and the horn alone (this can be done once and for once, because their dimension do not vary from one loudspeaker to another). Then, without unmounting the compression chamber, we add different acoustical loads to the compression chambers, and we compare the different measurements of the electrical impedance. This method is, in spirit, closed to those developed by Makarski and Behler [20,21] for their two-port "black-box model". These authors describe a model of loudspeaker similar to ours (described by Eqs. (1)–(3)). The difference is that the four elements of the matrix in Eq. (1) are not analytically related to the constitutive elements of the loudspeaker (e.g. mass of the moving element, length of wire, etc.), but rather written as unknown frequency-dependent functions, that have to be described numerically by measurements. By means of original measurement methods (acoustical impedance of a Kundt's tube loaded by the loudspeaker driver, electrical impedance of two coupled drivers, etc.) and boundary element simulations of the horn, they are able to measure numerically the four functions of the matrix. The tests show that this method is able to provide accurate predictions of the loudspeaker efficiency, for a wide variety of loudspeakers and horns, and for frequencies up to 20 kHz. However, since this model cannot lead to identify any lumped-element values, it cannot be used to modify the design of the loudspeaker constitutive elements.

4.1. Acoustical load parameters

The horn dimensions (r_t, r_m, and L) are estimated by geometrical means. To estimate the compression chamber parameters (V_{c0}, L_{c1}), we measure the acoustical input admittance of the compression chamber closed by a small pipe of length L_p, and we fit this measure to Eq. (B.1) (Appendix B).

4.2. Coupling factors ratio

Following Le Roux's work [55,56], the ratio S_d/Bl is estimated by measuring the loudspeaker electrical impedance, in two cases. In the first case, the loudspeaker is loaded by the closed compression chamber the equivalent volume of which is V_{eq}. In the second case, the compression chamber is closed by a cylindrical pipe of length L_p, section S_t which leads to an equivalent volumeV_{eq}^p. In both cases (as long as the moving element resonance frequency is far below the compression chamber first resonance frequency), we estimate the resonance parameters (resonance frequency ω_0 and quality factor Q_e), as well as the voice coil resistance R_e. From this estimations, we derive the coupling factor ratio S_d/Bl with

$$\frac{Bl}{S_d} = \sqrt{\rho c^2 \frac{L^p L^c}{(L^p - L^c)} \frac{V_{eq}^p}{V_{eq}\left(V_{eq} + V_{eq}^p\right)}}, \tag{16}$$

where L^c and L^p are the equivalent mechanical masses[3] and are estimated using

[3] Superscripted index c means "loaded with closed compression chamber".

$$L^{c} = \frac{R_{ec}}{\omega_0^{c} Q_e^{c}}, \tag{17a}$$

$$L^{p} = \frac{R_{ec}}{\omega_0^{p} Q_e^{p}}. \tag{17b}$$

Eq. (17) are drawn from the inversion of Eq. (B.4) (Appendix B).

4.3. Driver parameters

We estimate the driver parameters by measuring the input electrical impedance when the driver is loaded by the closed compression chamber. In this case, by fitting this measure to Eq. (B.2) (Appendix B), we estimate the closed chamber driver parameters (Q_m^c, Q_e^c, ω_0^c, ω_r, r, L_{ec}, and α). Finally the free-radiating driver parameters are evaluated by

$$Q_e = Q_e^c, \tag{18a}$$

$$\omega_0 = \omega_0^c \sqrt{1 - \frac{R_{ec}}{Q_e \omega_0^c} \frac{S_d^2}{(Bl)^2} \frac{\rho c^2}{V_{eq}}}, \tag{18b}$$

$$Q_m = Q_m^c \sqrt{1 - \frac{R_{ec}}{Q_e \omega_0^c} \frac{S_d^2}{(Bl)^2} \frac{\rho c^2}{V_{eq}}}. \tag{18c}$$

5. Model assessment

In this section, we apply the model and the parameter estimation method described above to a loudspeaker used as a new prototype of car horn. This allows us to validate the modelization of each element of the global model, and to evaluate the estimation method uncertainty. This loudspeaker has a membrane with a 5 cm diameter, and a 22 cm length horn (throat diameter: 2 cm, mouth diameter: 10 cm). The total weight of the device is 600 g.

5.1. Measurement settings

Parameter estimation requires both electrical and acoustical impedance measurements. All electrical impedances are measured with a 0.125 Ω resistor connected in series with the loudspeaker. Sweep measures are made with a Stanford Research SR785 analyzer. The loudspeaker is placed in an anechoic chamber. Electrical impedance measurements are compensated for wire transfert function. Accuracy is estimated at ±0.8% for impedance modulus, and ±0.1° for impedance phase. During measurements of both electrical impedance and loudspeaker efficiency, the loudspeaker is fed with a 10 mV input voltage, which ensures that the average total harmonic distortion is less than 1%. Acoustical impedances are measured with an impedance head described in [57,58]. Loudspeaker efficiency is measured by recording simultaneously pressure radiated at horn mouth and loudspeaker input voltage. Pressure is measured with a Sennheiser KE4 electret microphone (sensibility 153 mV/Pa).

5.2. Experimental determination of parameters

5.2.1. Compression chamber parameters

To estimate V_{c0} and L_{c1}, we measure the input acoustical impedance of the compression chamber closed by a

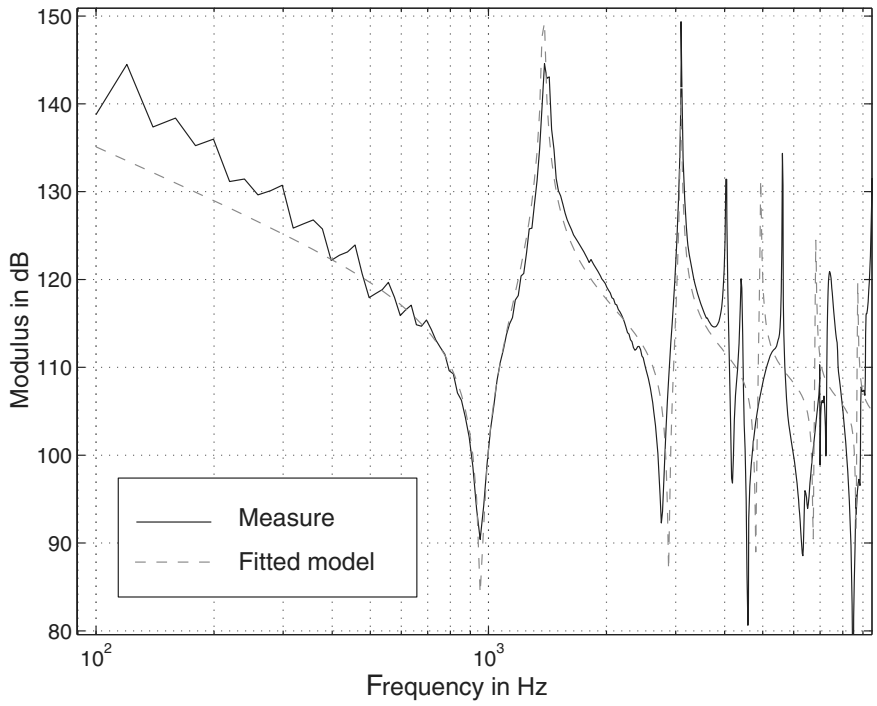

Fig. 5. Measured and predicted input acoustical impedance of the compression chamber loaded with a 60 mm long closed pipe.

60 mm long cylindrical pipe. The length of the pipe let the system resonance frequencies fall within the sensor bandwidth. A minimum least square fitting method is applied with 500 points between 100 Hz and 10 kHz (see Fig. 5). This figure shows that the two first measured resonance frequencies (sensor bandwidth) correspond to the predicted frequencies with an error smaller than the sensor accuracy, which validates our model. But the measured amplitudes are about 6 dB lower than the predicted ones. This error, greater than sensor accuracy, may be interpreted as viscothermal losses underestimation. Below 400 Hz, the measured slope is steeper than the predicted compliance behavior (−20 dB/decade). This may be due either to systematic failure of the measuring device at low frequencies, or to a phenomenon which is not taken into account in the model.

According to the fitting method confidence interval, this method allows to estimate V_{c0} with a precision of ±1.7% and L_{c1} with a precision of ±1.1%.

5.2.2. Horn parameters

First, the input acoustical impedance of the closed horn is studied in order to test the horn model without taking into account the radiation impedance. Within the sensor bandwidth, the differences between the estimated and the measured resonance frequencies are less than the sensor accuracy. The estimated resonance amplitude are 5 dB higher than the measured ones, which suggests that viscothermal losses are underestimated (see top panel of Fig. 6). Second, the impedance of the freely radiating horn is measured. Bottom panel of Fig. 6 shows that the model predictions and the measurements are consistant for the frequency domain [100 Hz to 2 kHz] indicating that the radiation impedance model is valid in this frequency range.

5.2.3. Coupling factor ratio

S_d/Bl is estimated by measuring the electrical impedance of the loudspeaker loaded with the closed compression chamber, and afterwards with the compression chamber terminated by a closed pipe (27.6 mm). Eq. (B.2) and measurements are fitted with Akabak software [52]. In order to evaluate the reproducibility errors, estimations are repeated 10 times. The standard deviation of the reproducibility error is ±1.6%.

5.2.4. Driver parameters

To estimate the driver parameters, we measure the electrical impedance of the loudspeaker with the closed compression chamber and fit it to Eq. (B.2) with Akabak software [52] (see Fig. 7). It can be noted that the compression chamber first resonance appears around 3.5 kHz. We repeat the estimation 10 times. The reproduciblity errors are listed in Table 1.

This shows that the mechanical quality factor Q_m^e is the most inaccurate value. This explains why Eq. (16) is based only on Q_e. The voice coil parameters f_r and L_{eb} estimations are also less accurate. Their estimation is biased by compression chamber modes. When we propagate this error to the estimation of the parameters for the freely radiating driver, we found that the most inacurrately estimated parameter is C_{mm}: ±6.0%.

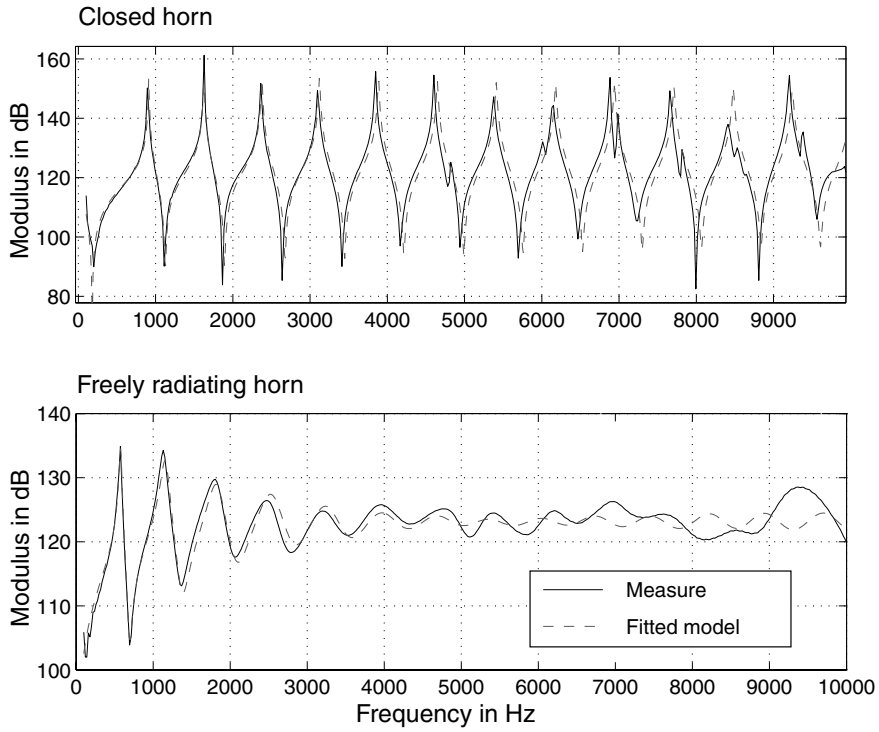

Fig. 6. Acoustical input impedance of the closed and of the freely radiating horn.

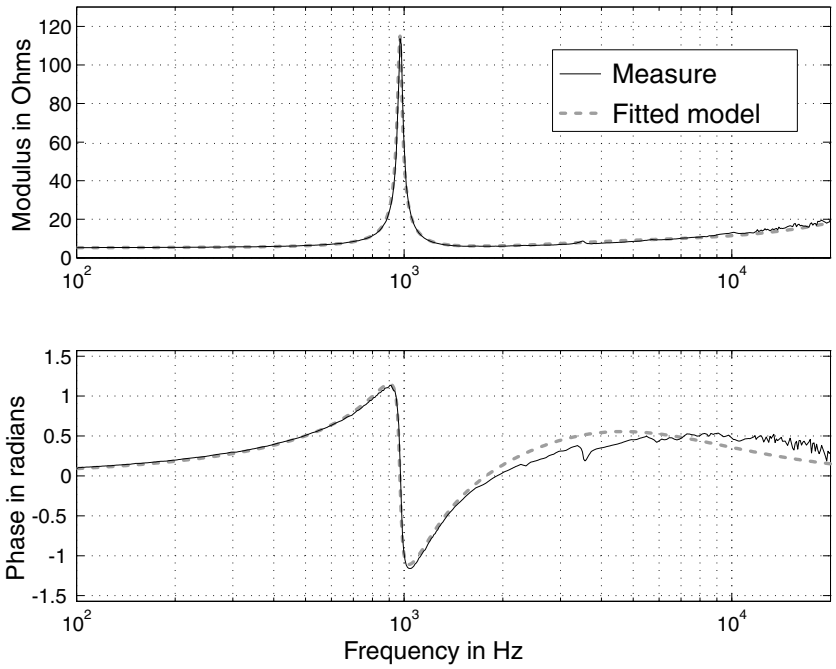

Fig. 7. Electrical impedance of the loudspeaker loaded with the closed compression chamber.

Table 1
Estimated reproducibility error of driver parameters, for the driver being loaded by the closed compression chamber

Parameter	Standard deviation[a] (%)	Parameter	Standard deviation[a] (%)
Q_m^c	4.2	R_{eb}^c	0.2
f_r^c	2.0	Q_e^c	0.2
L_{eb}^c	1.4	f_0^c	0.1
α^c	0.8	r^c	0.0

[a] % of average value.

5.3. Global model evaluation

We estimate the validity of the physical model developed in Section 3 by comparing the predicted and the measured electrical loudspeaker input impedances, and the predicted and the measured loudspeaker efficiencies (radiated pressure over input voltage). Measured and estimated efficiencies are reported in Fig. 8. For frequencies below 2.5 kHz, error between measured and predicted efficiency

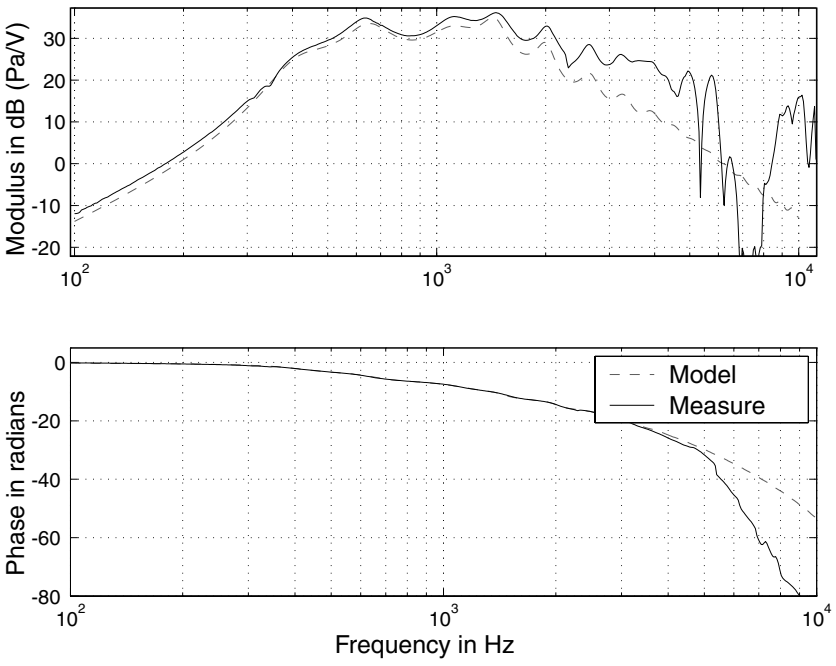

Fig. 8. Efficiency (mouth pressure over input voltage) of the free radiating loudspeaker.

is less than 2 dB. For frequencies between 2.5 kHz and 5 kHz, error is about 10 dB. Around 5 kHz and 7 kHz the measured response dramatically drops from the predicted one. Hence the predictions of the model are usable for frequencies below 2.5 kHz. For frequencies above 2.5 kHz, the radiation impedance model fails.

6. Discussion

In this paper, we have proposed a model using 14 parameters for describing the horn loudspeaker made of an electrodynamic driver coupled together with a compression chamber and a horn. The model is globally defined by a quadripole equation and a boundary condition. This formulation allows to easily express any desired quantity. We have defined a method that allows to estimate these parameters without unmounting the compression chamber, which would change the mechanical characteristics of the loudspeaker. The method is based on electrical impedance measurements of the loudspeaker loaded by different acoustic volumes. It needs to estimate the compression chamber equivalent volume when the driver is unmounted.

We have applied this model and the estimation method to a loudspeaker used as a new car horn. Due to confidentiality restrictions, we are not allowed to disclose here the numerical values of the estimated parameters. However, the modelization of each element fits rather well with the measured quantities. The estimation reproducibility errors are estimated of a few percents.

This model, and the associated parameter estimation method, suffers however from several drawbacks. Electrical and mechanical driver parameters have to be estimated with a curve fitting technique based on a measure of electrical impedance. To let the fitting algorithm converge, we need to simplify the models. While the loudspeaker behavior is fairly predicted by these simplified models for low frequencies, higher frequency response is clearly, although on a small amount, influenced by the compression chamber resonance modes. Our model is theoretically able to take this effect into account. This would however result in an over-parametrized model, that would make the curve fitting algorithm unable to converge.

The acoustic models of both compression chamber and conical horn used in this study fit the experimental data only for a limited bandwith up to 3.5 kHz, and so is limited the prediction ability of the global model. Within this bandwidth, the model predictions are closed to measurements. More precise models are available for compression chamber [59] and for horn (chaining small cylindrical elements to fit the precise bore geometry and better estimate viscothermal losses [36]), but the main limitation results from the radiation impedance model. A solution would be to generalize Helie's work [33] to our cone dimensions.

Then, this model allows to predict the loudspeaker linear behavior. Globally, this device acts like a band-pass filter. Its bandwith is approximatively 500 Hz to 2 kHz. This is rather narrow, since our previous work has recommended that car horns fundamental frequency must lie around 400 Hz, and sounds have to have a rich spectral content. Hence, loudspeaker design has to be reviewed to increase bandwith. Our model allows to predict how some device modifications may help to reach this goal. This model also allows to inverse-filter signal to compensate for loudspeaker response at high frequencies. This is, however, not possible for low frequencies, because energy boost at low frequencies would dramatically increase distortion. Finally, this model allows to listen to the sounds that would really be emitted by the device, and not only the laboratory created sounds. Therefore, signal specifications can be tested directly on the sound that would be heard by road users.

This model, however, is a linear model that permits to predict signal linear filtering, but does not allow to predict harmonic and intermodulation distortions. As car horn signals are very loud signals, it can be assumed that non-linear phenomena occur when the loudspeaker is used as a car horn. Then, the next step will be to include the main non-linear phenomena in the loudspeaker model. However, care must be taken to design a non-linear model that would be easily related to physical parameters.

7. Conclusion

In the context of sound quality, car horn builders are attempting to create new sounds by means of synthesizers and electrodynamic horn loudspeakers. A previous study [3] has provided some sound design specifications, in order to create new sounds which are still perceived as warning messages. However, as the laboratory-designed sounds will be altered by the loudspeaker, the loudspeaker response must be included in the design process.

Based on the huge literature dealing with loudspeaker, and on both theoretical and empirical considerations, we have proposed a linear model with 14 parameters for this horn loudspeaker. The problem is formalized by a matrix equation and a boundary condition. To explicit each term of this system, we have further modelized impedances of the different loudspeaker elements, electrical, mechanical and acoustical. Our model is mainly based on Thiele and Small's model, geometrical modelization of the compression chamber and acoustical studies of wave propagation in horns. We have also designed a parameter estimation technique, which allows to estimate the model parameter values with methods that are easily implementable in an industrial context. Within our loudspeaker bandwith (500 Hz to 2 kHz), this model is able to fairly predict the loudspeaker behavior.

Acknowledgements

This study has been founded by SCE Klaxon and by the french ministry of industry. The authors thank Jean-Pierre Dalmont at the Laboratoire d'Acoustique de l'Université du Maine for fruitful discussions and for his help in mea-

Table A.1
Glossary of symbols

Symbol	Analogy	
ρ	–	Air density
c	–	Sound velocity
B	–	Air-gap flux density
l	–	Length of voice coil wire
S_d	–	Effective area of the diaphragm
u_g	–	Generator voltage
i_g	–	Voice coil current
v_d	–	Diaphragm velocity
q_d	–	Volume velocity in front of diaphragm
p_d	–	Pressure at acoustical load
p_t	–	Pressure at horn throat
p_m	–	Pressure at horn mouth
Z_{ec}	Elec.	Voice-coil impedance
R_{ec}	Elec.	Voice-coil resistance
L_{ec}	Elec.	Voice-coil inductance
ω_r	–	Empirical parameters to
r	–	characterize voice-coil
α	–	impedance
Z_{mm}	Mech.	Motional impedance
Z_{em}	Elec.	Motional impedance
Z_{eM}	Elec.	Motional impedance including acoustical load
R_{mm}	Mech.	Mechanical losses
C_{mm}	Mech.	Suspensions compliance
M_{mm}	Mech.	Moving element mass
ω_0	–	Resonance pulsation of the moving element
Q_m	–	Quality ratio of the moving element
Z_{al}	Ac.	Input impedance of the acoustical load
Y_{al}	Ac.	Input admittance of the acoustical load
Z_{el}	Elec.	Input impedance of the acoustical load
C_{al0}	Ac.	Compliance equivalent to an air volume V_{eq0}
Z_{at}	Ac.	Horn throat impedance
Z_{hp}	Elec.	Loudspeaker input impedance
Z_{ar}	Ac.	Radiation impedance
C_{ac0}	Ac.	Compliance of air volume V_{c0}
ζ_t	Ac.	Charactristic impedance at throat
T^{pipe}	Ac.	Transmission function in a pipe
T^{horn}	Ac.	Transmission function in the horn

Table A.2
Glossary of geometrical symbols

Symbol	
S_d	Diaphragm projected section
V_c	Compression chamber equivalent volume
V_{c0}	Volume equivalent to the fluid layer between diaphragm and phase plug
V_{c1}	Volume equivalent to the volume between phase plug and compression chamber walls
V_{eq}	Volume équivalent to the compression chamber
V_{eq}^p	Volume équivalent to the compression chamber loaded with a pipe
L_{c1}	Length of cylindrical pipe of section S_g and volume equivalent to V_{c1}
L_p	Length of loading pipe
S_p	Section of loading pipe
V_p	Volume of loading pipe
r_t	Radius of horn throat
S_t	Section at horn throat (or compression chamber mouth)
r_m	Radius at horn mouth
S_m	Section at horn mouth
x_t, x_m, L	Horn dimensions

suring acoustical impedances, and two anonymous reviewers for their comments on previous versions of this article.

Appendix A. A symbols notation

Table A.1 and Table A.2

Appendix B. Loudspeaker loaded with a small cylindrical pipe

B.1. Acoustical impedance

When the compression chamber is loaded by a short cylindrial pipe of same section S_t and length L_p, Eq. (7) becomes[4]

$$Y_{al}^{p} = jC_{ac0}\omega + \frac{1}{\zeta_t} j\tan\left[k(L_{c1}+L_p)\right], \tag{B.1}$$

where $C_{ac0} = V_{c0}/\rho c$ is the acoustical compliance equivalent to volume V_{c0}. The input acoustical impedance of the closed-pipe loaded compression chamber exhibits then maxima and minima (resonance) for frequencies $\omega_n = (2n+1)\frac{\pi c}{2(L_{c1}+L_p)}$. Below the first resonance frequency, compression chamber behaves like a pure acoustical compliance, equivalent to an air volume $V_{eq} = V_{c0} + V_{c1} + S_t L_p$.

B.2. Loudspeaker electrical impedance

Below compression chamber first resonance frequency, loudspeaker electric input impedance may be approximated by Eq. (B.2)

$$Z_{hp}^{p} = R_{ec}\frac{Q_m^p}{Q_e^p}\frac{j\frac{\omega}{\omega_0^p}Q_m^{p\,-1}}{1 + j\frac{\omega}{\omega_0^p}Q_m^{p\,-1} + \left(j\frac{\omega}{\omega_0^p}\right)^2} + R_{ec}(1+\omega/\omega_r)^r + j(\omega L_{ec})^l \tag{B.2}$$

with

$$R^p = \frac{Bl^2}{R_{mm}}, \tag{B.3a}$$

$$C^p = \frac{M_{mm}}{Bl^2}, \tag{B.3b}$$

$$\frac{1}{L^p} = \frac{1}{Bl^2 C_{mm}} + \frac{S_d^2}{Bl^2 C_{eq}}, \tag{B.3c}$$

and

$$\omega_0^p = \frac{1}{\sqrt{L^p C^p}}, \tag{B.4a}$$

$$Q_m^p = \omega_0 R^p C^p, \tag{B.4b}$$

$$Q_e^p = \omega_0 R_{eb} C^p, \tag{B.4c}$$

[4] Superscript index ^{p} means "loaded with a closed pipe".

R^p, C^p, and L^p are, respectively, mechanical equivalent losses, compliance and mass.

References

[1] United Nation Organization, Economic and Social Council. Uniform provisions concerning the approval of audible warning devices and of motor vehicles with regard to their audible signals; 2000. Regulation 28 to the TRANS/WP.29/343/Rev.13 agreement. http://www.unece.org/trans/.

[2] Eargle J, Gander M. Historical perspectives and technology overview of loudspeakers for sound reinforcement. In: Proceedings of the 25th international AES convention, London, UK, June 2004. p. 412–32.

[3] Lemaitre G, Susini P, Winsberg S, McAdams S. Perception of the timbre of car horns. In: Proceedings of the Forum Acusticum Sevilla 2002, 2002. Abstract published in Acta Acustica united with Acustica, vol. 88; 2002. p. S123 (A).

[4] Lemaitre G, Susini P, Winsberg S, McAdams S. Perceptively based design of new car horn sounds. In: Proceedings of the international conference on Auditory Displays (ICAD), Boston, MA, USA, July 2003.

[5] Lemaitre G, Susini P, Winsberg S, McAdams S. The sound quality of car horns: Psychoacoustical study of timbre. Acta Acustica [Submitted for publication, manuscript code: AAA2005_415].

[6] Olson HF. Analysis of the effects of nonlinear elements upon the performance of a back-enclosed, direct radiator loudpseaker mechanism. J Audio Eng Soc 1962;10(2):156–62.

[7] Cunningham WJ. Non-linear distortion in dynamic loudspeakers due to magnetic effects. J Acoust Soc Am 1949;21(3):202–7.

[8] Gander MR. Dynamic linearity and power compression in moving-coil loudspeakers. J Audio Eng Soc 1986;34(9):627–46.

[9] Bequin P, Morfey CL. Weak nonlinear propagation of sound in a finite exponential horn. J Acoust Soc Am 2001;109(6):2649–59.

[10] Goldstein S, McLachlan NW. Sound waves of finite amplitude in an exponential horn. J Acoust Soc Am 1935;6:275–8.

[11] Klippel W. Modeling the nonlinearities in horn loudspeakers. J Audio Eng Soc 1996;44(6):470–80.

[12] Thiele AN. Loudspeakers in vented boxes. Proc IRE Aust 1961;22:487–508. Reprinted in the J Audio Eng Soc 1971;19:382–92.

[13] Small RH. Direct-radiator loudspeakers systems analysis. IEEE Trans Audio Electroacoust 1971;AU-19:269–81. Reprinted in the J Audio Eng Soc 1972;20(6):271–83.

[14] Small RH. Simplified louspeaker measurements at low frequencies. Proc Instit Radio Electron Eng (IREE) 1971;32:299–304. Reprinted in the J Audio Eng Soc 1972;20(1):28.

[15] Beranek LL. Acoustics. American Institute of Physics, for the Acoustical Society of America; 1954.

[16] Olson HF. Acoustical engineering. D. Van Nostrand Company Inc.; 1957.

[17] Keele Jr DB. Low-frequency loudspeaker assessment by nearfield sound-pressure measurement. J Audio Eng Soc 1974;22(4).

[18] Klippel W. Dynamic measurement and interpretation of the nonlinear parameters of electrodynamic loudspeakers. J Audio Eng Soc 1990;38(12):944–55.

[19] Murphy DJ. Axisymmetric model of a moving-coil loudspeaker. J Audio Eng Soc 1993;41(9):679–90.

[20] Behler GK, Makarski M. Two-port representation of the junction between horn driver and horn. In: Proceedings of the 111th convention of the audio engineering society, New York, USA, September 2001, Convention paper 5409.

[21] Makarski M. Determining two-port parameters of horn drivers using only electrical measurements. In: Proceedings of the 116th convention of the audio engineering society, Berlin, Germany, May 2004, Convention paper 6098.

[22] Suzuki H. Sound radiation from a concave or convex dome in a semi-infinite tube. J Audio Eng Soc 1985;33(12):1956–62.

[23] Leach Jr WM. Loudspeaker voice-coil inductance losses: circuit models, parameter estimation, and effect on frequency response. J Audio Eng Soc 2002;50(6):442–50.

[24] Knudsen MH, Jensen JG. Low-frequency loudspeaker models that include suspension creep. J Audio Eng Soc 1993;41(1/2):3–18.

[25] Bruneau A-M, Bruneau M. Electrodynamical loudspeaker with baffle: motional impedance and radiation. J Audio Eng Soc 1986;34(12):970–80.

[26] Nederveen CJ. Acoustical aspects of musical instruments. Nothern Illinois University Press; 1969. Revised edition 1991.

[27] Webster AG. Acoustical impedance and the theory of horns and of the phonograph. Proc Natl Acad Sci 1919:275–82. Reprinted in the J Audio Eng Soc 1977;25(1/2):24–8.

[28] Eisner E. Complete solutions of the Webster horn equation. J Acoust Soc Am 1967;41(4, pt. 2):1126–46.

[29] Levine H, Schwinger J. On the radiation of sound from an unflanged circular pipe. Phys Rev 1948;73(4).

[30] Caussé R, Kergomard J, Lurton X. Input impedance of brass musical instruments. Comparison between experiment and numerical method. J Acoust Soc Am 1984;75(1):241–54.

[31] Dalmont J-P, Nederveen C, Joly N. Radiation impedance of tubes with different flanges: numerical and experimental investigations. J Sound Vib 2001;244(3):505–33.

[32] Norris AN, Sheng IC. Acoustic radiation form a circular pipe with an infinite flange. J Sound Vib 1989;135:85–93.

[33] Hélie T, Rodet X. Radiation of a pulsating portion of a sphere: application to horn radiation. Acta Acust United Acust 2003;89:565–76.

[34] Benade AH, Jansson EV. On plane and spherical waves in horns with nonuniform flare. I. Theory of radiation, resonance frequencies, and mode conversion. Acustica 1974;31(2):79–98.

[35] Jansson EV, Benade AH. On plane and spherical waves in horns with nonuniform flare. II. Prediction and measurements of resonance frequencies and radiation losses. Acustica 1974;31(4):185–202.

[36] Plitnik GR, Strong WJ. Numerical method for calculating input impedances of the oboe. J Acoust Soc Am 1979;65(3):816–25.

[37] Holland KR, Fahy F, Morfey C. Prediction and measurement of the one-parameter behavior of horns. J Audio Eng Soc 1991;39(May):315–37.

[38] Kergomard J. General equivalent circuits for acoustic horns. J Audio Eng Soc 1988;36(12):948–54.

[39] Smith JO. Physical modeling using digital waveguides. Comput Music J 1992;16(4). Available at: http://www-CCRMA.stanford.edu/jos/.

[40] Hanna CR, Slepian J. The function and design of horns for loudspeakers. Trans Am Instit Electr Eng 1924;43. Reprinted in the J Audio Eng Soc 1977;25(9).

[41] Plach DJ. Design factors in horn-type speakers. J Audio Eng Soc 1953;1(3):1–5.

[42] Keele Jr DB. Optimum horn mouth size. In: AES Preprint no: 933 (B7); 1973. Presented at the 46th convention of the audio engineering society, September 10–13, 1973.

[43] Olson HF. The action of a direct radiator loudspeaker with a non-linear cone suspension system. J Acoust Soc Am 1944;16(1):1–4.

[44] Johansen TF. On the directivity of horn loudspeakers. J Audio Eng Soc 1994;42(December):1008–19.

[45] Smith BH. An investigation of the air chamber of horn type loudspeakers. J Acoust Soc Am 1953;25(2):305–12.

[46] Henricksen CA. Phase plug modelling and analysis: circumferential versus radial types. In: 55th convention of the audio engineering society; 1976. AES Preprint no: 1140(M5).

[47] Leach Jr WM. On the specification of moving-coil drivers for low-frequency horn-loaded loudspeakers. J Audio Eng Soc 1979;27(12):950–9.

[48] Geddes E, Clark D. Computer simulation of horn-loaded compression drivers. J Audio Eng Soc 1987;35(7/8):556–66.

[49] Vanderkooy J. A model of loudspeaker driver impedance incorporating Eddy currents in the pole structure. J Audio Eng Soc 1989:119–27.

[50] Wright JR. An empirical model for loudspeaker motor impedance. J Audio Eng Soc 1990;38(10):749–54.
[51] Vanderkooy J, Boers PM, Aarts RM. Direct-radiator loudspeaker systems with high *Bl*. J Audio Eng Soc 1990;51(7/8):625–6342003.
[52] Panzer JW. Akabak – an electroacoustic simulator. In: Proceedings of the IOA conference on reproduced sound, Windermer GB, October 1996. http://www.akabak.de.
[53] Schurer H, Berkhoff AP, Slump CH, Herrmann OE. Modeling and compensation of nonlinear distortion in horn loudspeakers. J Audio Eng Soc 1995;43(7/8):592–8. Engineering Report.
[54] Kergomard J. Ondes quasi-stationnaires dans les pavillons avec pertes visco-thermiques aux parois: calcul de l'impédance. Acustica 1981;48:31–43.
[55] Le Roux J-C. Le haut-parleur électrodynamique: estimation des paramétres électroacoustiques aux basses fréquences et modélisation de la suspension. PhD thesis, Laboratoire d'Acoustique de l'Université du Maine; 1994.
[56] Herzog P, Le Roux J-C. Modélisation basses fréquences d'un haut-parleur électrodynamique. In: Journal de Physique IV. Colloque C5, supplément au Journal de Physique III, vol. 4, mai 1994; 1994. p. 225–8.
[57] Dalmont J-P, Bruneau A-M. Acoustic impedance measurement: plane-wave mode and first helical mode contributions. J Acoust Soc Am 1991;91(5).
[58] Kergomard J, Garcia A, Tagui G, Dalmont JP. Analysis of higher order mode effect in an expansion chamber using modal theory and equivalent electrical circuit. J Sound Vib 1989;129(3):457–75.
[59] Skvor Z. Vibrating systems and their equivalent circuits. Elsevier; 1991, ISBN 0-444-98806-8.